



Review

Radiomics and artificial intelligence: General notions and applications in the carotid vulnerable plaque

Roberta Scicolone^a, Sebastiano Vacca^b, Francesco Pisu^a, John C. Benson^c, Valentina Nardi^d, Giuseppe Lanzino^e, Jasjit S. Suri^f, Luca Saba^{a,*}

^a Department of Radiology, Azienda Ospedaliero-Universitaria (A.O.U.), di Cagliari—Polo di Monserrato, Cagliari, Italy

^b University of Cagliari, School of Medicine and Surgery, Cagliari, Italy

^c Department of Radiology, Mayo Clinic, Rochester, MN, USA

^d Department of Cardiovascular Medicine, Mayo Clinic, Rochester, MN, USA

^e Department of Neurosurgery, Mayo Clinic, Rochester, MN, USA

^f Stroke Monitoring and Diagnostic Division, AtheroPoint™, Roseville, CA, USA



ARTICLE INFO

Keywords:

Radiomics

Artificial intelligence

Machine learning

Carotid

Cerebrovascular events

Carotid vulnerable plaque

Stroke

ABSTRACT

Carotid atherosclerosis plays a substantial role in cardiovascular morbidity and mortality.

Given the multifaceted impact of this disease, there has been increasing interest in harnessing artificial intelligence (AI) and radiomics as complementary tools for the quantitative analysis of medical imaging data. This integrated approach holds promise not only in refining medical imaging data analysis but also in optimizing the utilization of radiologists' expertise. By automating time consuming tasks, AI allows radiologists to focus on more pertinent responsibilities. Simultaneously, the capacity of AI in radiomics to extract nuanced patterns from raw data enhances the exploration of carotid atherosclerosis, advancing efforts in terms of (1) early detection and diagnosis, (2) risk stratification and predictive modeling, (3) improving workflow efficiency, and (4) contributing to advancements in research.

This review provides an overview of general concepts related to radiomics and AI, along with their application in the field of carotid vulnerable plaque. It also offers insights into various research studies conducted on this topic across different imaging techniques.

1. Introduction

Carotid atherosclerosis is a condition characterized by the narrowing or blockage of the carotid arteries. This is often caused by the buildup of fatty deposits on the walls of the arteries, which can lead to stroke [1] and dramatically increases the risk of cardiovascular morbidity and mortality [2].

Although manual evaluation is crucial in radiology, it is limited by the naked eye, with the possibility of overlooking small or early-stage abnormalities, subjective interpretation, and variations in individual expertise. Radiomics and artificial intelligence (AI) can serve as complementary tools in this context, by automatically assessing several quantitative variables across the full image collection, potentially

detecting subtle patterns or information that may not be readily apparent through manual review alone.

The integration of radiologists' experience with the computational capabilities of AI and radiomics has the potential to boost diagnosis accuracy, improve efficiency, and reveal insights in medical imaging data that would otherwise go unnoticed. Incorporating these advanced technologies into the radiologist's clinical practice can result in more thorough and accurate assessments, thereby enhancing patient care [3]. Here we will review the use of radiomics and AI in the evaluation of carotid plaques.

Abbreviations: AI, Artificial Intelligence; AUC, Area Under the Curve; CAD, Computer-Aided Diagnosis; CT, Computed Tomography; DL, Deep learning; FC, Fibrous Cap; IPH, Intraplaque Hemorrhage; k-NN, k-Nearest Neighbour; LASSO, Least Absolute Shrinkage and Selection operator; LR, Logistic Regression; LRNC, Lipid Rich Necrotic Core; ML, Machine Learning; MRI, Magnetic Resonance Imaging; SVM, Support Vector Machine; US, Ultrasound.

* Corresponding author.

E-mail address: lucasaba@tiscali.it (L. Saba).

<https://doi.org/10.1016/j.ejrad.2024.111497>

Received 16 March 2024; Received in revised form 14 April 2024; Accepted 3 May 2024

Available online 6 May 2024

0720-048X/© 2024 Elsevier B.V. All rights reserved.

2. Radiomics

Radiomics pertains to the extraction and analysis of quantitative features from medical imaging data with the goal of converting them into usable data, allowing for a more detailed and comprehensive understanding of the underlying pathology and potentially providing valuable information about disease's characteristics, prognosis, and treatment responses.[4,5] The typical steps involved in a pipeline utilizing radiomic features are summarized in Fig. 1.

Despite the lack of consensus concerning the definition, nomenclature, evaluation algorithm, and classification of quantitative imaging features—which complicates the comparison of various radiomics studies—these features can be nonetheless classified into morphology-based, statistics-based, model-based and transform-based (see Supplementary Table 1 for definitions of the various categories) [6,7]. A list of morphological-based features and statistics-based features according to the Imaging Biomarker Standardization Initiative (IBSI) [8] is presented in Supplementary Tables 2 and 3, respectively.

3. Artificial intelligence

AI encompasses the creation of algorithms and computational models that imitate human intellect in order to carry out particular tasks. In the field of medical imaging, AI techniques, including machine learning (ML) and deep learning (DL), are employed to examine extensive collections of medical images [9].

In general terms, AI, ML, DL represent hierarchically related concepts, with AI being an umbrella term encompassing various techniques that allow computer programs to learn from experience and replicate human thought processes for solving complex and varied tasks.

ML is one of the approaches to AI and it refers to the ability of a computer system to acquire knowledge about a domain by identifying patterns in multidimensional raw data without being explicitly programmed to do so [9]. Different ML paradigms exist, for instance:

- Supervised learning [7,10], which involves training an algorithm using a dataset that is labeled, meaning that each input data point is

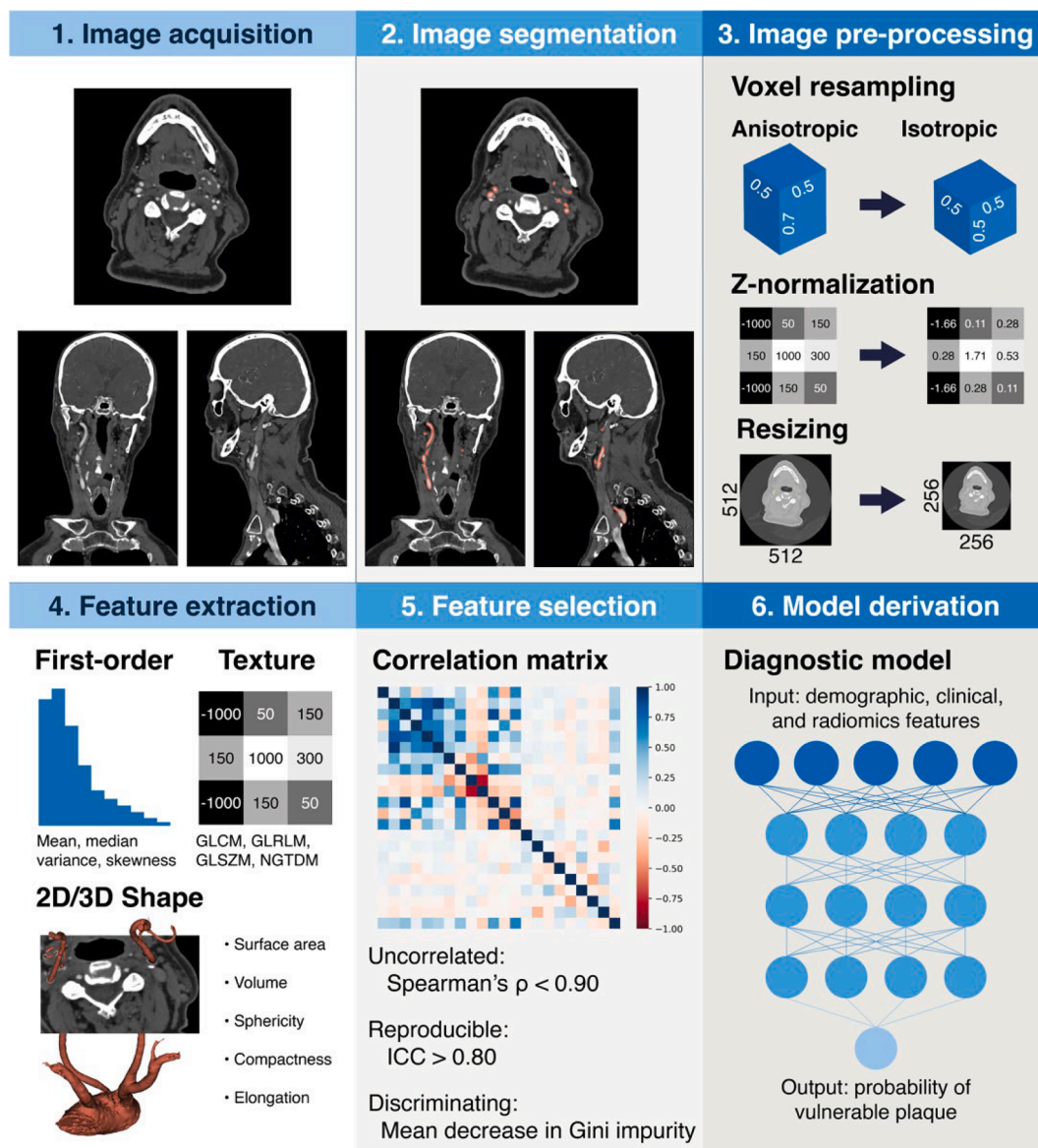


Fig. 1. Typical steps involved in a pipeline utilizing radiomic features. Initially, images are acquired (1), followed by the isolation of regions-of-interest (ROIs) (2). Subsequently, both the image and the segmentation masks undergo preprocessing, including feature normalization, wherein features are scaled to balance their numerical range (3) before several radiomic features are extracted from the ROIs (4). These features are often selected based on criteria such as being uncorrelated, reproducible, and possessing diagnostic capabilities (5). Finally, a diagnostic model is constructed using these features (6).

associated with a matching output label. The objective is for the algorithm to acquire the ability to understand the relationship between the input and output, enabling it to provide predictions for novel, unobserved data (Fig. 2A).

- Unsupervised learning [7,10], which refers to the process of analyzing unlabeled data in order to identify patterns, correlations, or structures without any explicit supervision from the algorithm. The system acquires knowledge from the intrinsic organization of the supplied data (Fig. 2B).

Hybrid paradigms [11] also exist, including semi-supervised learning and self-supervised learning.

DL is a sub-field of ML that mainly employs artificial neural networks to model and solve a variety of tasks. The term “deep” relates to the usage of deep neural networks, which comprise several layers (hence the name “deep”) of linked nodes, also known as neurons [12]. An example of neural network is represented in Fig. 3.

DL has substantially boosted the state-of-the-art in many fields, resulting in breakthroughs in previously difficult problems for classic ML algorithms. Unlike traditional ML, which often requires the manual

crafting of task-specific features, DL excels in automatically learning complex representations from data given its ability to process the raw data directly. This is particularly advantageous in contexts where pre-determining relevant features is challenging, and manual feature extraction is both time-consuming and reliant on expert knowledge. This paradigm, known as representation learning, is fundamental to DL [7,13].

Common architectures for image-related tasks include convolutional neural networks, which typically involve convolutional layers, pooling layers, and fully connected components [12,13].

The U-Net, introduced by Ronneberger and colleagues in 2015, is a particular type of convolutional neural network that has been specifically developed for the purpose of performing semantic segmentation tasks in the field of image processing. The method gained significant popularity in the field of biological image analysis, as well as in other domains that demand accurate segmentation at the pixel level [14,15].

Although the original U-Net design achieved success, it had specific limitations, for instance in addressing the problems of over-segmentation and under-segmentation [15]. To overcome these challenges, the no-new-net or nnU-Net, emerged as the cutting-edge

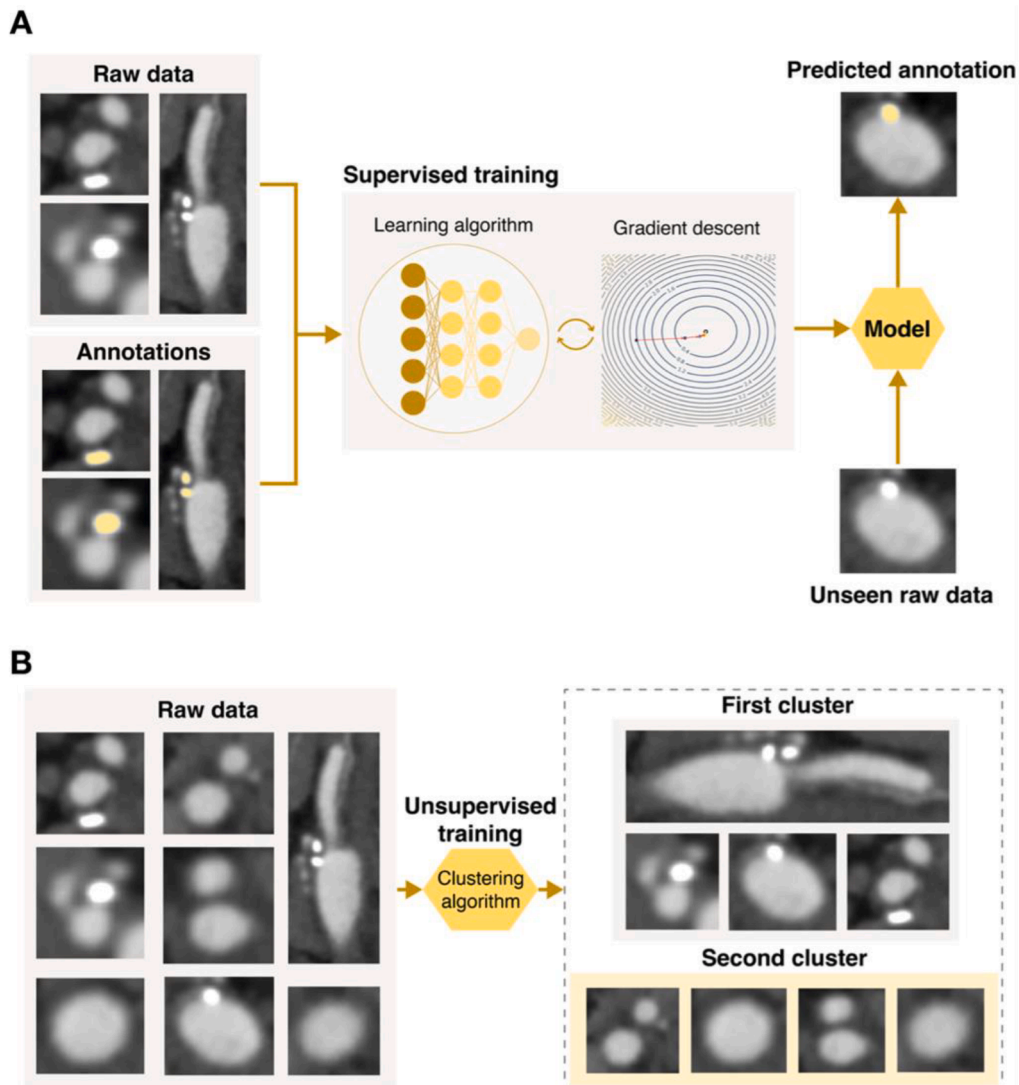


Fig. 2. Schematic representation of supervised and unsupervised learning. In supervised learning, raw data with expert annotations are utilized to derive a model by training a learning algorithm, commonly employing gradient descent, wherein the model’s weights are iteratively adjusted to closely match the ground-truth data. Once trained, the model can be used to predict unseen data. In panel A, the model is trained and utilized to segment calcified carotid plaques. In unsupervised learning, data without annotations are inputted to an unsupervised model to learn intrinsic properties of the data, typically through the use of a clustering algorithm. In panel B, the model is employed to stratify the raw data into two clusters of carotid plaques, one with calcified plaques and one without.

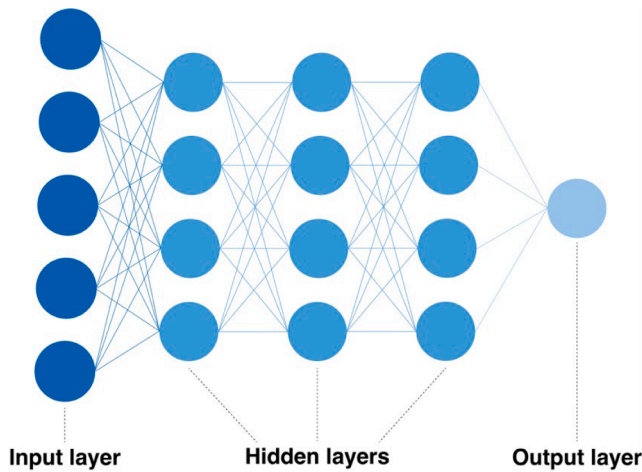


Fig. 3. Schematic representation of a feed-forward neural network. In feed-forward neural networks, input data undergo processing through a sequence of hidden layers, each comprising multiple neurons. These layers work to extract progressively abstract and high-level features. This process involves projecting the input features into a latent space. By condensing this latent space into output neurons, it becomes feasible to calculate the desired quantity based on the specific task being addressed. Tasks may include classification, semantic segmentation, or regression.

framework for medical image analysis tasks. Unlike prior DL architectures, highly specific and requiring manual selection of model design elements, nnU-Net is an automated deep learning-driven segmentation system that automatically adjusts its settings, such as preprocessing, network design, training, and postprocessing. This showcases the capacity to adjust to new datasets autonomously, constantly surpassing several earlier techniques without the need for operator intervention [16].

4. Imaging features of plaque vulnerability

In the past, the degree of carotid arterial stenosis was considered the main factor for evaluating the severity of stroke risk, mostly shaped by research dating back to the 1980–90, which emphasized the efficacy of carotid endarterectomy (CEA) in patients with significant stenosis (ranging from 70 % to 99 %) [17,18].

Nevertheless, a growing body of evidence indicates that identifying unstable plaque characteristics might significantly enhance the assessment of carotid atherosclerosis in both symptomatic and asymptomatic patients: the majority of patients with severe carotid stenosis are actually asymptomatic, with a rate of symptomatic conversion at <1 % per year; on the other hand, a significant number of patients with <50 % stenosis experience anterior circulation stroke [19–24].

To further on this topic, in October 2023, the Carotid Plaque RADS was introduced by Saba and colleagues [25], providing a reliable multi-imaging scoring reporting system to assess the risk of cerebrovascular events based on carotid plaque morphology [26,27].

More precisely, the Carotid Plaque RADS (Fig. 4) considers:

- Imaging characteristics: maximum wall thickness, lipid-rich necrotic core (LRNC), intraplaque hemorrhage (IPH), rupture of the fibrous cap (FC), and intraluminal thrombus;
- Ancillary features: positive carotid remodeling, plaque burden, stenosis progression, carotid plaque calcifications;
- Modifiers: limited diagnostic study, stents, and prior carotid endarterectomy.

Ultrasound (US), being widely available and non-invasive, can be used to assess plaque burden [25,29]. US can also detect the presence of a thick FC, the latter presenting as a hyperechoic structure and being the indicator of the score 3a, whereas in the presence of juxta-luminal black areas, representing either LRNC with a thin FC (score 3b), plaque rupture (score 4b) or intraluminal thrombus (score 4c), further imaging is necessary.

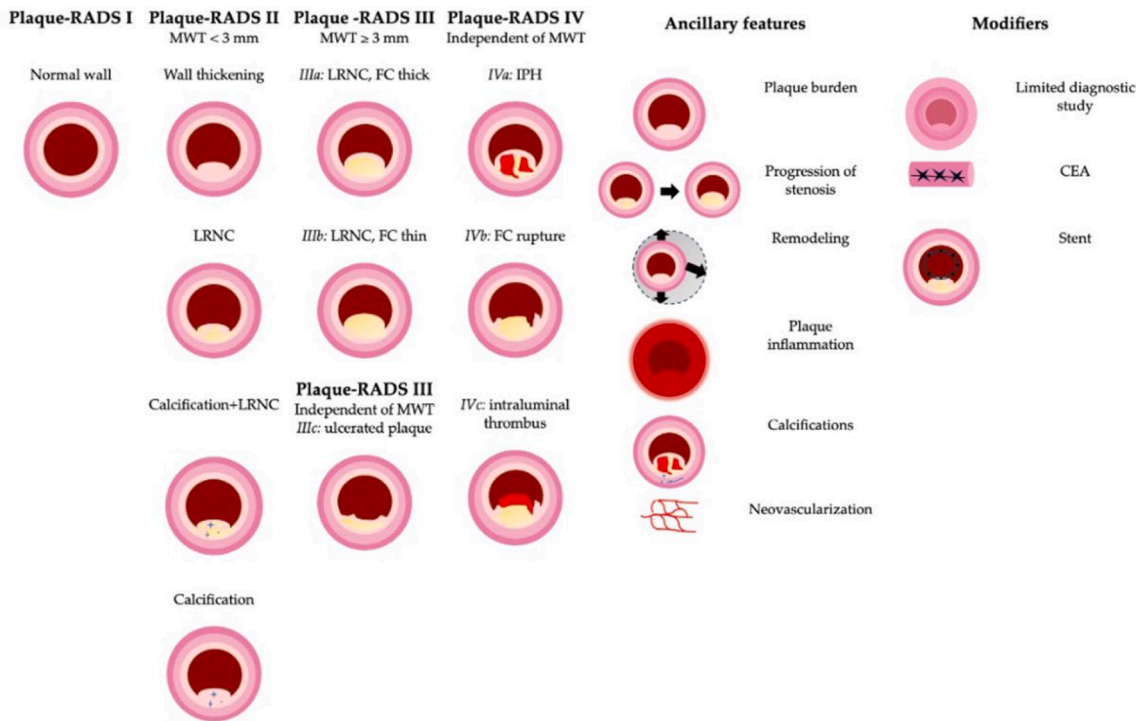


Fig. 4. Schematic representation of the different Carotid Plaque RADS categories. Reproduced with permission from Saba et al. [28] Presentation concept based on Saba et al. [25]. Abbreviations: LRNC: Lipid-Rich Necrotic Core; FC: Fibrous Cap, MWT: Mean Wall Thickness, IPH: Intraplaque Hemorrhage, CEA: Carotid Endarterectomy.

In this scenario, computed tomography (CT), as highlighted by the latest consensus statement [30], serves as the benchmark non-invasive imaging method for assessing plaque ulcerations, defined as contrast material that protrudes from the vascular lumen into the plaque for at least 1 mm. However, due to plaque calcifications and its inability to accurately detect FC thickness and/or integrity, magnetic resonance imaging (MRI) is the best imaging technique to detect surface irregularities [25,31,32].

Beside plaque surface morphology, plaque composition, referring to the types and distribution of various components within the plaque, including LRNC, fibrous tissue, calcifications, IPH, and inflammation, is an important factor in determining plaque vulnerability [25]. Both CT and US are limited in the evaluation of plaque composition. US, as stated before, cannot properly differentiate between LRNC and IPH. The main limitation of CT techniques is a substantial overlap of Hounsfield unit values among LRNC, fibrous tissues, and IPH. Additionally, plaque calcifications, as mentioned before, can cause beam-hardening, edge-blur, and halo effect artifacts, limiting the CT's ability to determine plaque composition [33]. However, it is expected that photon-counting scanners may address some of the current limitations of conventional CT scanners [34,35].

MRI has proven to be highly accurate in the detection of features of vulnerability in carotid plaques. By employing a multi-sequence protocol (including T1-weighted, T2-weighted, proton density, and time-of-flight sequences) along with a specialized carotid coil, MRI can effectively identify significant characteristics such as the presence of a LRNC, thinning or rupture of the fibrous cap, and intraplaque hemorrhage IPH [33,36].

5. Radiomics and AI applications in the carotid vulnerable plaque

In the context of carotid artery disease, radiomics and AI can help in the automatic segmentation of the carotid plaques across all imaging modalities and in the detection of carotid plaque vulnerability features, especially for CT and MRI. The first aspect falls outside the purpose of this review, as it has already been addressed in a recent publication by Wang et al. [37]. Such advanced technologies can be applied to every diagnostic technique, including US, CT and MRI.

5.1. US

Mougiakakou et al. [38] created on a dataset of 54 symptomatic plaques and 54 asymptomatic plaques a computer-aided diagnosis (CAD) system to analyze US images of carotid arteries and classify them into symptomatic or asymptomatic based on their echogenicity characteristics. The system is composed of three modules. The first one, the feature extraction module, extracts first-order statistical features and Laws' texture energy features. Second, a dimensionality reduction module reduces the number of features using the analysis of variance. Third, the classifier module which consists of a neural network trained using a hybrid approach encompassing genetic algorithms and the back propagation algorithm. The hybrid method was also compared with a neural network trained using the traditional back propagation algorithm only. The patients were equally distributed between the training set ($n = 54$, 27 symptomatic and 27 asymptomatic), the validation set ($n = 27$, 14 symptomatic and 13 asymptomatic) and in the testing set ($n = 27$, 13 symptomatic and 14 asymptomatic). The hybrid method performed better with areas under the curve (AUC) for both training and validation sets equal to 1. In the testing set, the proposed approach achieved an AUC of 0.973; the classical method exhibited AUCs of 1, 0.931 and 0.918 in the training, validation, and testing sets, respectively.

Lo and colleagues [39] in 2022 created a CAD system using histogram, shape, and texture features on a cohort including 102 symptomatic and 75 asymptomatic patients, with a total of 513 S and 458 normal carotid color doppler CCD images. A logistic regression (LR) algorithm was used

to integrate such features and derive a model to classify images into symptomatic or asymptomatic categories. The LR classifier was compared to the support vector machine (SVM) and k-nearest neighbors (k-NN). LR outperformed both SVM and k-NN, achieving accuracies of 87 %, 60 %, and 87 % when separately using histogram, shape, and texture features, respectively. Additionally, the combined model achieved even better performance, with an accuracy of 89 % and an AUC 0.94.

Zhang et al. [40] tested the performance of US-based texture analysis combined with least absolute shrinkage and selection operator (LASSO) regression to detect carotid plaque vulnerability. The overall cohort comprised 150 consecutive patients with suspected cerebrovascular events and randomized into the training ($n = 105$, 70 %) and testing ($n = 45$, 30 %) sets. A conventional diagnostic model proposed was constructed using four variables from conventional ultrasound (including surface morphology, FC state, plaque echo, and plaque ulcer formation) and it was combined with a texture-based model. In the training set, the combined ultrasound-texture feature model achieved an AUC of 0.88. Similarly, in the testing set, the proposed approach achieved an AUC of 0.87.

5.2. CT

In 2022, Zhang et al. [41] employed demographics and radiomic features to develop a clinical factor model for detecting IPH, utilizing the LASSO method. The authors retrospectively recruited a total of 46 patients with 106 carotid plaques that served as the training set, and an additional 18 patients with 38 plaques constituted the test set. The authors conducted a comparison between the model based solely on clinical variables, and a model based solely on radiomic features, and a combined model. In the clinical model, several variables were considered, including the degree of stenosis, maximum plaque thickness, and presence of ulceration. To construct the clinical factor model, initial univariable analysis was conducted to compare the differences in these clinical factors between symptomatic and asymptomatic groups. Subsequently, a multiple logistic regression analysis was performed using statistically significant variables from the univariable analysis as inputs. Notably, the degree of luminal stenosis emerged as the sole independent predictor in the clinical factor model. The results demonstrated the superiority of the combined model, with the AUC significantly higher than that of the clinical factor model in both the training (0.743) and external test sets (0.811). Furthermore, the nomogram exhibited satisfactory predictive efficacy with good calibration.

Similarly, Xia et al. [42] developed ML models for predicting the risk of transient ischemic attack in patients with mild carotid artery stenosis. A total of 179 patients, with 34 presenting symptoms and 145 without symptoms, were randomized into training set ($n = 165$) and testing sets ($n = 65$). Five classification algorithms were used to train models on a selection of radiomic features, including random forest, eXtreme Gradient Boosting, LR, SVM, and k-NN. Three different models were derived: a clinical-only model including low-density lipoprotein and uric acid, a radiomic-only model, and combined model. The random forest model, constructed using radiomics and clinical feature information, exhibited the highest accuracy on both training (0.988) and testing sets (0.863), with corresponding AUC values of 0.983 and 0.879, respectively.

Another study published in 2023 by Shi and colleagues [43], retrospectively analyzed 167 patients, 70 with symptoms and 97 without symptoms to develop and validate a multivariable model incorporating conventional clinical and imaging characteristics and radiomic features for the assessment of plaque vulnerability. The conventional model included plaque ulceration, carotid rim sign as imaging features and homocysteine as clinical characteristic. The combined model demonstrated superior performance compared to both the conventional-only and radiomic-only models, achieving an accuracy of 0.784 in the training cohort and 0.761 in the testing cohort, with corresponding AUC

values of 0.856 and 0.832, respectively. Additionally, calibration analysis indicated a good fit between predicted and actual likelihood of stroke in both the training and validation cohorts. Decision curves analysis further highlighted the clinical utility of the combined model.

5.3. MRI

Zhang and colleagues [44] developed a ML based on MRI radiomics features and ML algorithm for the detection of vulnerable carotid plaques and compared its performance to a traditional model based on conventional MRI features. A total of 162 patients were included in the study and were randomized into training and testing sets. The traditional model was constructed using features related to IPH and LRNC identified through multivariable logistic regression analysis. The predictive radiomics model for identifying high-risk plaques comprised several steps: first, features were normalized to zero mean and standard deviation of 1; then, a feature selection algorithm based on statistical significance in univariable analysis ($p < 0.05$) and discriminatory ability ($AUC > 0.65$) was employed to select an initial set of features. Further reduction was achieved with the LASSO algorithm. The final set of 33 radiomic features were used to derive the radiomic model. The radiomic model demonstrated superior performance in both the training and testing sets, achieving AUC values of 0.988 and 0.984, respectively. In comparison, the traditional model yielded AUCs of 0.825 and 0.804 for the training and testing sets, respectively. Furthermore, when combining the radiomic and traditional models, the combined model exhibited even higher AUCs of 0.989 and 0.986 for the training and testing sets, respectively.

Another study published in 2023 [45] aimed to develop a 3D carotid plaque radiomics model based on high-resolution magnetic resonance imaging, to quantitatively identify vulnerable plaques. The cohort was composed by 48 symptomatic patients and 42 asymptomatic patients, divided in training and testing cohort. The radiomics model was compared to a traditional model based on IPH, plaque enhancement, wall remodeling pattern, and lumen stenosis. Results showed that the radiomics model outperformed the traditional model, with AUC values of 0.915 and 0.835 in the training and testing sets, respectively. In contrast, the traditional model achieved AUC values of 0.816 and 0.778 in the training and testing sets, respectively. The final combined model achieved AUC values of 0.957 and 0.864 in the training and testing set, respectively. The calibration curve showed a significant correlation between the diagnostic results of both the radiomic-only and combined models and the actual results in both sets. Additionally, decision curves analysis revealed a net benefit for patients with the combined and radiomic-only model in both the training and testing sets, confirming the usefulness of the developed nomogram in clinical practice.

A work conducted by Chen et al. [46], developed a radiomics-based MRI sequence from high-resolution magnetic resonance imaging, combined with clinical high-risk factor, to differentiate between symptomatic and asymptomatic plaques. They retrospectively enrolled 115 patients and randomized them into training ($n = 81$, 53 with symptomatic plaques and 28 with asymptomatic plaques) and test sets ($n = 34$, 22 with symptomatic plaques and 12 with asymptomatic plaques). T2-weighted imaging was used for segmentation and extraction of the texture features. Max-Relevance and Min-Redundancy and the LASSO algorithm were employed to optimize the model by selecting only the most relevant variables. The radiomic-only model (Radscore) was applied to construct a diagnostic model considering the texture features. Subsequently, the Radscore was compared with the clinical only and the combined models. In the clinical model, low- and high-density lipoprotein, their ratio, IPH and LRNC were included. Conversely, the combined model only included the ratio of low- and high-density lipoprotein, along with IPH and LRNC based on the minimal Akaike Information criterion. The combined model yielded the highest AUC of 0.929 in the training group and 0.912 in the test group. This difference was statistically significant compared to the clinical model ($p = 0.023$) and

Radscore ($p = 0.013$) in the training group, but not in the test group ($p = 0.090$ vs. $p = 0.155$). The Radscore did not show a significant difference from the clinical model in either the training group ($p = 0.782$) and the test group ($p = 0.852$).

An overview of previously published US, CT and MRI studies using radiomics and AI for the detection of carotid vulnerable plaque is shown in Table 1.

6. Current limitations

While radiomic and AI hold promise, particularly when integrated into CAD systems, they also poses several issues and concerns that demand attention and resolution.

6.1. Interpretability and explainability of AI model

Interpretability and explainability involve understanding and trusting model decisions, but they have distinct definitions:

- Interpretability refers to the degree to which an individual can understand the causal relationship between the input features, the model, and its predictions. In simpler terms, it involves ensuring that the decision-making process of the model is comprehensible and open to people. In medical ML, interpretability is crucial because healthcare practitioners need to trust the model's predictions and comprehend the underlying rationale [63,64].
- Explainability involves providing precise and explicit rationales or explanations for the individual predictions made by the model. The main objective is to offer explanations into the reasoning behind a model's specific conclusion about a given input. Doctors must have confidence in the overall performance of the model and comprehend the rationale behind each estimate [63,64].

Certain AI models possess a "black box" characteristic, indicating the presence of highly complex algorithms that are challenging for humans to understand. To address the significant difficulties posed by these black-box models, a growing body of research is dedicated to developing AI models that possess both explainability and interpretability [63–65].

6.2. Regulatory issues of AI

The issue of consent for data usage poses a significant challenge that is often overlooked by organizations providing commercial products [65–67].

There are different legislative models for privacy protection in using AI for healthcare [68]:

- For Europe, the legislative model employs regulations such as the EU Data Protection Directive of 1995 (95/46/EC) and the General Data Protection Regulation of 2018 (GDPR), to protect personal healthcare information together with other personal information in an integrated manner.
- For US, the Health Insurance Portability and Accountability Act of 1996 (HIPAA), the Standards for Privacy of Individually Identifiable Health Information of 2000 (commonly referred to as the Privacy Rule), and the Health Information Technology for Economic and Clinical Health Act (HITECH) of 2009, provide a systematic and nationwide framework for the protection of private health information.
- For China, the Personal Information Protection Law (PIPL) and the Civil Code.

All the aforementioned legislative models require consent for handling healthcare information and allow the individual the right to revoke consent, which can potentially impact the performance of the ML software [68].

Table 1

Previous US, CT and MRI studies regarding the application of radiomics and artificial intelligence model in the detection of carotid vulnerable plaque.

Authors	Imaging technique	Year and study design	Sample size	Study aim	Category of used radiomic features	ML/DL	Results
Mougiakakou et al. [38]	US	2007; retrospective	54 sym and 54 asym plaque images	Automatic classification of plaque images into sym and asym	First order statistical features LTE	Hybrid NN vs Classic NN	Hybrid neural network better with AUC = 1 in training and validation set and AUC = 0.973 in testing set; Acc = 100 % in training and validation set and 96.3 % in the testing set).
Lo et al. [39]	US	2022; retrospective	513 sym and 458 asym images from 102 sym and 75 asym patients	Automatic classification of plaque images into sym and asym	Morphological features First and second order statistical features	LR vs SVM vs k-NN	LR performed better for first, second order statistical features and all combined feature with Acc = 87, 87, 89 % respectively SVM and k-NN both performed better for morphological features with both Acc = 61 %
Zhang et al. [40]	US	2022; bidirectional	150 patients, 57 asym and 93 sym	Automatic classification of plaque images into sym and asym	First and second order statistical features Transform-based features Model-based features	LR vs Non radiomic	Combined model better with AUC = 0.88 for training and AUC = 0.87 testing set
Acharya et al. [47]	US	2013; retrospective	<u>UK</u> : 346 plaque images, 196 sym and 150 asym <u>Portugal</u> : 146 plaque images, 44 sym and 102 asym	Automatic classification of plaque images into sym and asym	Second order statistical features Transform-based features	SVM DT Fuzzy GMM k-NN NBC	<u>Portugal dataset</u> Fuzzy better with Acc = 93.1 <u>UK dataset</u> : SVM-RBF better with Acc = 85.3
Acharya et al. [48]	US	2012; retrospective	<u>Plaque dataset (UK)</u> : 346 images, 150 asym and 196 sym <u>Wall dataset (HK + Italy)</u> : 342 images: -300 HK asym - 42 Italy: 22 sym and 20 asym	Automatic classification of plaque and wall images into asym and sym	LBP LTE	<u>Plaque dataset</u> : SVM vs DT vs GMM vs k-NN vs NBC vs RBPNN vs Sugeno fuzzy <u>Wall dataset</u> : SVM vs k-NN vs RBPNN	<u>Plaque dataset</u> : SVM poly 2 better with Acc = 83 <u>Wall dataset</u> : Without IMTV _{poly} : KNN and RBPNN with Acc = 88.6 With IMTV _{poly} : any with Acc = 89.5
Acharya et al. [49]	US	2012; prospective	346 plaque images, 150 asym and 196 sym	Automatic classification of plaque images into asym and sym	First and second order statistical features	Adaboost vs SVM	SVM RBF performed better with Acc = 82.4
Acharya et al. [50]	US	2012; retrospective	146 plaques, 102 asym and 44 sym, from 99 patients	Automatic classification of plaque images into asym and sym	First and second order statistical features Wavelet transform features Radon transform features HOS	SVM	SVM RBF performed better with Acc = 91.7
Chaudhry et al. [51]	US	2016; retrospective	300 images	Automatic segmentation and classification of carotid arteries in normal and abnormal	First order statistical features	SVM vs KNN vs MLBPNN	SVM with Acc = 98.84
Huang et al. [52]	US	2022; prospective	548 plaques, 381 sym and 167 asym	Automatic classification of plaque images into asym and sym	First and second order statistical based features	MLR vs Non radiomic	Final nomogram better with an AUC = 0.927 in the training cohort and AUC = 0.919 in the test cohort
Kyriacou et al. [53]	US	2006; retrospective	274 plaques, 137 sym and 137	Automatic classification of plaque images into asym and sym	DST	SVM vs PNN	SVM with correct classifications score of 66.7 %
Kyriacou et al. [54]	US	2011; prospective	1121 patients	Risk stratification based on ultrasonic plaque texture features and clinical features	First and second order statistical features FDTA FPS	LR	AUC = 0.834 94.7 % correct classification
Lambrou et al. [55]	US	2012; retrospective	274 plaque images, 137 sym and 137	Automatic classification of plaque images into asym and sym	First, second and high order statistical based features Morphological	ANN ANN-CP SVM SVM-CP NBC	k-NN(Acc = 70,43) k-NN-CP(Acc = 70.8)

(continued on next page)

Table 1 (continued)

Authors	Imaging technique	Year and study design	Sample size	Study aim	Category of used radiomic features	ML/DL	Results
Latha et al. [56]	US	2021; retrospective	361 images, 202 normal images and 159 plaque images	Automatic classification into presence or absence of plaque	features LTE FDTA FPS Morphology features First, second and high order statistical features LBP FDTA	NBC-CP k-NN k-NN-CP NBC vs DLVQ	DLVQ better, on the selected features Acc = 91.68, on all the extracted Acc = 88.72
Smitha et al. [57]	US	2019; retrospective	96 images	Automatic classification of plaque images into asym and sym	Second order statistics-based features	SVM	SVM-RBF best performance by combining contrast, correlation, energy and homogeneity: Acc = 100 % with RBF of 0.3 and 0.1
Tsiaparas et al. [58]	US	2011; retrospective	20 plaques, 11 sym and 9 asym	Automatic classification of plaque images into asym and sym	Statistics-based texture features Wavelet transform features Fractal texture features	SVM vs PNN	SVM better with Acc = 70
Huang et al. [59]	US	2015; prospective	275 plaques, 85 hyperechoic, 83 intermediate and 100 anechoic	Classify carotid plaque echogenicity	First order and second order statistical features Wavelet transform features Model-Based Features	k-NN	k-NN MDFs better with AUC = 0.918 for identifying anechoic plaques
Pedro et al. [60]	US	2013; prospective	146 plaques from 99 patients, 30 sym and 69 asym	Automatic classification of plaque images into asym and sym	First order statistical features Wavelet transform features	MLR	AUC = 77
Zhang et al. [41]	CT	2022 retrospective	46 patients with 106 plaques in the training set (46 with IPH and 60 without) and 18 patients with 38 plaques in the testing set (18 with IPH and 20 without)	Differentiation of carotid plaques with intraplaque hemorrhage	First order and second order statistical features Wavelet transform features	MLR vs Non radiomic	Radiomics nomogram better with AUC = 0.743–0.811 in the training and testing cohort, respectively
Xia et al. [42]	CT	2023 retrospective	179 patients, 34 sym and 145 asym, total 219 plaques	Predict the risk of transient ischemic attack in patients with mild carotid stenosis	First and second order statistics based features	Non radiomic vs Best radiomic (RF, XGB LR, SVM, K-NN)	RF combined better with AUC = 0.983–0.879 in the training and testing set, respectively
Shi et al. [43]	CT	2023 retrospective	167 patients, 70 sym and 97 asym	Assess plaque vulnerability	Wavelet transform features First and second order statistics features	MLR vs Non radiomic	Combined better with AUC = 0.856–0.832 in the training and testing set, respectively
Le et al. [61]	CT	2021 retrospective	41 patients, 82 plaques, 41 sym plaques, 41 asym plaques	Test feature robustness and to identify culprit and non-culprit arteries	First, second and high order statistics-based features	Calcium only vs best radiomic (Elastic Net, LR, XGB)	Radiomics + calcium better with AUC = 0.73
Acharya et al. [62]	CT	2013 retrospective	20 patients, 11 sym and 9 asym, 200 sym images and 200 asym images	Automatic classification of plaque into asym and sym	LBP Wavelet transform features	SVM	SVM-RBF better with Acc = 88
Zhang et al. [44]	MRI	2021 retrospective	162 patients, 108 sym and 54 asym. 121 in the training set (81 sym + 40 asym) and 41 in the test cohort (17 sym + 14 asym)	Automatic classification of plaque into asym and sym	Morphology features Second order statistics-based features Wavelet transform features	LR vs MLR and Non radiomic	Combined better with AUC = 0.989–0.986 in the training set and in the testing set, respectively
Zhang et al. [45]	MRI	2023 retrospective	90, 48 sym and 42 asym	Quantitatively identify vulnerable plaques	Morphology features First and second order features Wavelet transform features	MLR vs Non radiomic	Combined better with AUC = 0.957–0.864 in the training and testing set, respectively
Chen et al. [46]	MRI	2023 retrospective	115 patients, 75 sym and 40 asym	Differentiating sym from asym carotid plaques	Wavelet transform features First order and second order statistics features	MLR rad vs Non radiomic	Combined better with AUC = 0.929–0.912 in the training and testing set, respectively

Abbreviations: *Sym*: Symptomatic; *Asym*: Asymptomatic; *Acc*: Accuracy; *LTE*: Law's Texture Energy; *NN*: Neural Network; *AUC*: area under the curve; *LR*: Linear regression; *SVM*: Support Vector Machine; *k-NN*: k-Nearest Neighbour; *DT*: Decision Tree; *GMM*: Gaussian Mixture Model; *IMTV*: Intima-Media Thickness Variability; *RBPNN*: Radial Basis Probabilistic Neural Network; *HOS*: High Order Spectra; *NBC*: Naïve Bayes Classifier; *LBP*: Local Binary Pattern; *MLBPNN*: Machine Learning-Based Back Propagation Neural Networks; *MLR*: Multiple Linear Regression; *DLVQ*: Dynamic learning vector quantization; *FDTA*: Fractal dimension texture analysis; *DST*: Discrete Size Transform; *PNN*: Probabilistic Neural Network; *FPS*: Fourier Power Spectrum; *ANN*: Artificial Neural Network; *CP*: Conformal Predictor; *MDF*: Most Discriminative Features; *RF*: Random Forest; *XGB*: eXtreme Gradient Boosting.

Additionally, it is important to note that, at least in Europe, there is currently no public database available to verify the certification or clinical validation of AI-based software [66]. Finally, there is legislative uncertainty around liability in healthcare, both in the US and Europe, concerning the application of AI. This uncertainty poses a risk of insufficient insurance coverage in cases of harm resulting from inaccurate predictions made by AI, potentially limiting the practical value of such software [67,69].

6.3. Repeatability and reproducibility of radiomic features

A common approach to feature extraction relies on the computation of image biomarkers or features within a region of interest, such as mean intensity, volume, and texture heterogeneity. However, each feature is affected differently by variations in scanner type, acquisition settings, patient positioning, image reconstruction algorithms, and the specific approach employed for delineating the region of interest. If radiomic models include characteristics that are not robust to such changes, their performance will be subpar when applied to novel data, affecting their generalizability [70].

Repeatability and reproducibility are crucial aspects of features reliability in radiomics. Repeatability refers to the consistency in achieving identical results when conducting the same analysis on the same subject, under identical conditions, and using the same imaging parameters. In contrast, reproducibility focuses on the ability to obtain the same features from different parameters and experimental conditions [6,71–73].

Test-retest imaging is often used to identify non-robust image characteristics, by imaging the same region of interest multiple times within a short time interval usually with the same acquisition protocol. This approach allows for identification of non-robust features, as the imaging sets are similar but not identical. Subsequently, non-robust features are excluded from further analysis [74]. While it is crucial to identify reliable characteristics, conducting test-retest imaging for every radiomic investigation poses challenges due to the need for extra resources, such as staff, imaging time, and radiation dosage, as well as the difficulty in achieving generalizability. Moreover, feature robustness is dependent on the specific phenotype being studied and the imaging modality used, making it challenging to extrapolate information on feature robustness from research involving multiple phenotypes and modalities [74,75].

6.4. Model validation and model generalizability

Due to potential issues with the representativeness and preparation of training data, any trained model, even if it has passed internal validation (where a portion of the dataset is used for training and the rest for validation), should be considered potentially non-generalizable and therefore undergo, prior to deployment in a real-world scenario, external validation, which involves testing the model with new data that were not included in the original input data or are significantly different. This way, data derived from entirely distinct sources have limited similarities, yet they may nevertheless have valuable characteristics. A well-trained model that captures useful aspects will consistently provide favorable outcomes even when faced with novel data repeatedly [76].

7. Future perspectives

Based on the aforementioned studies, it is evident that radiomics and AI will become essential components of a radiologist's routine. Further

technological progress will enable the development of increasingly sophisticated algorithms to stratify the risk of stroke based on features of plaque instability, as well as monitor treatment response. By integrating radiomics features with clinical data and even other “-omics” data, the performance of AI models will undoubtedly be enhanced [77].

8. Conclusions

The integration of AI, radiomics and clinical data into the field of medical imaging, with a special focus on carotid atherosclerosis, holds significant promise and potentially can improve clinical practice. By automating repetitive tasks and reducing inter-observer variability, AI-based CAD systems can optimize radiologist's efficiency, allowing them to allocate more time to patient care. Furthermore, AI's ability to identify nuanced patterns in imaging data presents opportunities for early detection and diagnosis of adverse plaque characteristics, leading to improved risk stratification for cerebrovascular events. As we continue to explore the capabilities of AI in medical imaging, its integration into clinical workflows stands to greatly enhance patient outcomes and advance the field of vascular medicine.

Finally, within medical research, these technologies facilitate large-scale analysis of imaging and clinical data, thereby aiding in the discovery of new patterns, biomarkers, and associations pertinent to carotid artery disease. Consequently, these technological advancements have the potential to enhance the accuracy and efficiency of medical image analysis, ultimately leading to improved outcomes for individuals affected by carotid artery disease.

Nevertheless, it is critical to prioritize the reproducibility and repeatability of the selected radiomic features, while also upholding fair and ethical practices in AI utilization, particularly concerning patient consent in the research studies. Additionally, comprehensive algorithm validation, coupled with efforts in the development of interpretable and explainable models and in the optimization of model performance to enhance therapeutic value without compromising patient safety, are paramount.

Only by addressing all these critical issues can we ensure the regular and safe implementation of radiomics and AI into routine clinical practice.

CRediT authorship contribution statement

Roberta Scicolone: . **Sebastiano Vacca**: Writing – review & editing, Writing – original draft, Conceptualization. **Francesco Pisu**: Writing – review & editing, Writing – original draft, Conceptualization. **John C. Benson**: Writing – review & editing, Writing – original draft, Conceptualization. **Valentina Nardi**: Writing – review & editing, Writing – original draft, Conceptualization. **Giuseppe Lanzino**: Writing – review & editing, Writing – original draft, Conceptualization. **Jasjit S. Suri**: Writing – review & editing, Writing – original draft. **Luca Saba**: .

Declaration of competing interest

The authors declare that they have no known competing financial interests or personal relationships that could have appeared to influence the work reported in this paper.

Appendix A. Supplementary material

Supplementary data to this article can be found online at <https://doi.org/10.1016/j.ejrad.2024.111497>.

[org/10.1016/j.ejrad.2024.111497](https://doi.org/10.1016/j.ejrad.2024.111497).

References

- [1] S.C. Bir, R.E. Kelley, Carotid atherosclerotic disease: a systematic review of pathogenesis and management, *Brain Circ.* 8 (3) (2022) 127–136, <https://doi.org/10.4103/bc.bc.36.22>.
- [2] R. Ornello, D. Degan, C. Tiseo, et al., Distribution and temporal trends from 1993 to 2015 of ischemic stroke subtypes: a systematic review and meta-analysis, *Stroke* 49 (4) (2018) 814–819, <https://doi.org/10.1161/STROKEAHA.117.020031>.
- [3] A. Ibrahim, S. Primakov, M. Beuque, et al., Radiomics for precision medicine: Current challenges, future prospects, and the proposal of a new framework, *Methods* 188 (2021) 20–29, <https://doi.org/10.1016/j.ymeth.2020.05.022>.
- [4] J.E. Van Timmeren, D. Cester, S. Tanadini-Lang, H. Alkadhi, B. Baessler, Radiomics in medical imaging—“how-to” guide and critical reflection, *Insights Imag.* 11 (1) (2020) 91, <https://doi.org/10.1186/s13244-020-00887-2>.
- [5] B. Koçak, E.Ş. Durmaz, E. Ateş, Ö. Kılıçkesmez, Radiomics with artificial intelligence: a practical guide for beginners, *Diagn. Interv. Radiol.* 25 (6) (2019) 485–495, <https://doi.org/10.5152/dir.2019.19321>.
- [6] M.E. Mayerhoefer, A. Materka, G. Langs, et al., Introduction to radiomics, *J. Nucl. Med.* 61 (4) (2020) 488–495, <https://doi.org/10.2967/jnumed.118.222893>.
- [7] M. Kolossváry, C.N. De Cecco, G. Feuchtnner, P. Maurovich-Horvat, Advanced atherosclerosis imaging by CT: radiomics, machine learning and deep learning, *J. Cardiovasc. Comput. Tomogr.* 13 (5) (2019) 274–280, <https://doi.org/10.1016/j.jctt.2019.04.007>.
- [8] A. Zwanenburg, M. Vallières, M.A. Abdalah, et al., The image biomarker standardization initiative: standardized quantitative radiomics for high-throughput image-based phenotyping, *Radiology* 295 (2) (2020) 328–338, <https://doi.org/10.1148/radiol.2020191145>.
- [9] M.K. Santos, J.R. Ferreira Júnior, D.T. Wada, A.P.M. Tenório, M.H.N. Barbosa, P.M. A. de Marques, Artificial intelligence, machine learning, computer-aided diagnosis, and radiomics: advances in imaging towards to precision medicine, *Radiol. Bras.* 52 (6) (2019) 387–396, <https://doi.org/10.1590/0100-3984.2019.0049>.
- [10] R.C. Deo, Machine learning in medicine, *Circulation* 132 (20) (2015) 1920–1930, <https://doi.org/10.1161/CIRCULATIONAHA.115.001593>.
- [11] S. Bhattacharyya, D. Konar, J. Platos, C. Kar, K. Sharma (Eds.), *Hybrid Machine Intelligence for Medical Image Analysis*, Springer Nature, 2020.
- [12] P.M. Cheng, E. Montagnon, R. Yamashita, et al., Deep learning: an update for radiologists, *Radiographics*. 41 (5) (2021) 1427–1445, <https://doi.org/10.1148/rq.2021200210>.
- [13] S.F. Ahmed, M.S.B. Alam, M. Hassan, et al., Deep learning modelling techniques: current progress, applications, advantages, and challenges, *Artif. Intell. Rev.* 56 (11) (2023) 13521–13617, <https://doi.org/10.1007/s10462-023-10466-8>.
- [14] O. Ronneberger, P. Fischer, T. Brox, U-Net: Convolutional Networks for Biomedical Image Segmentation. Published online May 18, 2015. Accessed September 8, 2023. <<http://arxiv.org/abs/1505.04597>>.
- [15] N. Siddique, P. Sidike, C. Elkin, V. Devabhaktuni, U-Net and its variants for medical image segmentation: theory and applications, *IEEE Access* 9 (2021) 82031–82057, <https://doi.org/10.1109/ACCESS.2021.3086020>.
- [16] F. Isensee, P.F. Jaeger, S.A.A. Kohl, J. Petersen, K.H. Maier-Hein, nnU-Net: a self-configuring method for deep learning-based biomedical image segmentation, *Nat. Methods*. 18 (2) (2021) 203–211, <https://doi.org/10.1038/s41592-020-01008-z>.
- [17] G.G. Ferguson, M. Eliasziv, H.W.K. Barr, et al., The North American symptomatic carotid endarterectomy trial: surgical results in 1415 patients, *Stroke* 30 (9) (1999) 1751–1758, <https://doi.org/10.1161/01.STR.30.9.1751>.
- [18] Randomised trial of endarterectomy for recently symptomatic carotid stenosis: final results of the MRC European Carotid Surgery Trial (ECST). *The Lancet*. 351 (9113) (1998) 1379–1387. doi:10.1016/S0140-6736(97)09292-1.
- [19] M. O'Brien, A. Chandra, Carotid revascularization: risks and benefits, *Vasc Health Risk Manag.* 10 (2014) 403–416, <https://doi.org/10.2147/VHRM.S48923>.
- [20] A. Kocczak, A. Schindler, D. Sepp, et al., Complicated carotid artery plaques and risk of recurrent ischemic stroke or TIA, *J. Am. Coll. Cardiol.* 79 (22) (2022) 2189–2199, <https://doi.org/10.1016/j.jacc.2022.03.376>.
- [21] A.L. Abbott, Extra-cranial carotid artery stenosis: an objective analysis of the available evidence, *Front Neurol.* 13 (2022) 739999, <https://doi.org/10.3389/fneur.2022.739999>.
- [22] T.G. Brott, J.L. Halperin, S. Abbara, et al., 2011 ASA/ACCF/AHA/AANN/AAAS/ACR/ASNR/CNS/SAIP/SCAI/SIR/SNIS/SVM/SVS Guideline on the Management of Patients With Extracranial Carotid and Vertebral Artery Disease: Executive Summary: A Report of the American College of Cardiology Foundation/American Heart Association Task Force on Practice Guidelines, and the American Stroke Association, American Association of Neuroscience Nurses, American Association of Neurological Surgeons, American College of Radiology, American Society of Neuroradiology, Congress of Neurological Surgeons, Society of Atherosclerosis Imaging and Prevention, Society for Cardiovascular Angiography and Interventions, Society of Interventional Radiology, Society of NeuroInterventional Surgery, Society for Vascular Medicine, and Society for Vascular Surgery, *Circulation* 124 (4) (2011) 489–532, <https://doi.org/10.1161/CIR.0b013e31820d8d78>.
- [23] S. Shahidi, A. Owen-Falkenberg, U. Hjerpested, A. Rai, K. Ellemann, Urgent best medical therapy may obviate the need for urgent surgery in patients with symptomatic carotid stenosis, *Stroke* 44 (8) (2013) 2220–2225, <https://doi.org/10.1161/STROKEAHA.111.000798>.
- [24] M. Venermo, G. Wang, A. Sedrakyan, et al., Editor's choice – carotid stenosis treatment: variation in international practice patterns, *Eur. J. Vasc. Endovasc. Surg.* 53 (4) (2017) 511–519, <https://doi.org/10.1016/j.ejvs.2017.01.012>.
- [25] L. Saba, R. Cau, A. Murgia et al., Carotid Plaque-RADS, a novel stroke risk classification system, *JACC Cardiovasc Imaging*. Published online September 29, 2023:S1936-878X(23)00431-X. doi:10.1016/j.jcmg.2023.09.005.
- [26] L. Saba, T. Saam, H.R. Jäger, et al., Imaging biomarkers of vulnerable carotid plaques for stroke risk prediction and their potential clinical implications, *Lancet Neurol.* 18 (6) (2019) 559–572, [https://doi.org/10.1016/S1474-4422\(19\)30035-3](https://doi.org/10.1016/S1474-4422(19)30035-3).
- [27] L. Saba, W. Brinjikji, J.D. Spence, et al., Roadmap consensus on carotid artery plaque imaging and impact on therapy strategies and guidelines: an international, multispecialty, expert review and position statement, *AJNR Am J Neuroradiol.* 42 (9) (2021) 1566–1575, <https://doi.org/10.3174/ajnr.A7223>.
- [28] L. Saba, R. Scicolone, E. Johansson, et al., Quantifying carotid stenosis: history, current applications, limitations, and potential: how imaging is changing the scenario, *Life.* 14 (1) (2024) 73, <https://doi.org/10.3390/life14010073>.
- [29] A.N. Nicolaides, A.G. Panayiotou, M. Griffin, et al., Arterial ultrasound testing to predict atherosclerotic cardiovascular events, *J. Am. Coll. Cardiol.* 79 (20) (2022) 1969–1982, <https://doi.org/10.1016/j.jacc.2022.03.352>.
- [30] L. Saba, C. Loewe, T. Weikert, et al., State-of-the-art CT and MR imaging and assessment of atherosclerotic carotid artery disease: standardization of scanning protocols and measurements—a consensus document by the European Society of Cardiovascular Radiology (ESCR), *Eur. Radiol.* 33 (2) (2022) 1063–1087, <https://doi.org/10.1007/s00330-022-09024-7>.
- [31] R. Sztajzel, S. Momjian, I. Momjian-Mayor, et al., Stratified gray-scale median analysis and color mapping of the carotid plaque: correlation with endarterectomy specimen histology of 28 patients, *Stroke* 36 (4) (2005) 741–745, <https://doi.org/10.1161/01.STR.0000157599.10026.ad>.
- [32] C.C. Mitchell, J.H. Stein, T.D. Cook, et al., Histopathologic validation of grayscale carotid plaque characteristics related to plaque vulnerability, *Ultrasound Med. Biol.* 43 (1) (2017) 129–137, <https://doi.org/10.1016/j.ultrasmedbio.2016.08.011>.
- [33] L. Saba, N. Agarwal, R. Cau, et al., Review of imaging biomarkers for the vulnerable carotid plaque, *JVS-Vasc. Sci.* 2 (2021) 149–158, <https://doi.org/10.1016/j.jvssci.2021.03.001>.
- [34] A. Shami, J. Sun, C. Gialeli, et al., Atherosclerotic plaque features relevant to rupture-risk detected by clinical photon-counting CT ex vivo: a proof-of-concept study, *Eur. Radiol. Exp.* 8 (2024) 14, <https://doi.org/10.1186/s41747-023-00410-4>.
- [35] A. Meloni, F. Cademartiri, V. Positano, et al., Cardiovascular applications of photon-counting CT technology: a revolutionary new diagnostic step, *J. Cardiovasc. Dev. Dis.* 10 (9) (2023) 363, <https://doi.org/10.3390/jcdd10090363>.
- [36] J.S. McNally, M.S. McLaughlin, P.J. Hinchley et al., Intraluminal Thrombus, Intraplaque Hemorrhage, Plaque Thickness, and Current Smoking Optimally Predict Carotid Stroke.
- [37] Y. Wang, Y. Yao, Application of artificial intelligence methods in carotid artery segmentation: a review, *IEEE Access* 11 (2023) 13846–13858, <https://doi.org/10.1109/ACCESS.2023.3243162>.
- [38] S.Gr. Mougialakou, S. Golemati, I. Gousias, A.N. Nicolaides, K.S. Nikita, Computer-aided diagnosis of carotid atherosclerosis based on ultrasound image statistics, Laws' texture and neural networks, *Ultrasound Med. Biol.* 33 (1) (2007) 26–36, <https://doi.org/10.1016/j.ultrasmedbio.2006.07.032>.
- [39] C.M. Lo, P.H. Hung, Computer-aided diagnosis of ischemic stroke using multi-dimensional image features in carotid color Doppler, *Comput. Biol. Med.* 147 (2022) 105779, <https://doi.org/10.1016/j.combiomed.2022.105779>.
- [40] L. Zhang, Q. Lyu, Y. Ding, C. Hu, P. Hui, Texture analysis based on vascular ultrasound to identify the vulnerable carotid plaques, *Front Neurosci.* 16 (2022) 885209, <https://doi.org/10.3389/fnins.2022.885209>.
- [41] S. Zhang, L. Gao, B. Kang, X. Yu, R. Zhang, X. Wang, Radiomics assessment of carotid intraplaque hemorrhage: detecting the vulnerable patients, *Insights Imag.* 3 (1) (2022) 200, <https://doi.org/10.1186/s13244-022-01324-2>.
- [42] H. Xia, L. Yuan, W. Zhao, et al., Predicting transient ischemic attack risk in patients with mild carotid stenosis using machine learning and CT radiomics, *Front Neurol.* 14 (2023) 1105616, <https://doi.org/10.3389/fneur.2023.1105616>.
- [43] J. Shi, Y. Sun, J. Hou et al., Radiomics signatures of carotid plaque on computed tomography angiography: an approach to identify symptomatic plaques, *Clin. Neuroradiol.* Published online May 17, 2023. 10.1007/s00062-023-01289-9.
- [44] R. Zhang, Q. Zhang, A. Ji, et al., Identification of high-risk carotid plaque with MRI-based radiomics and machine learning, *Eur. Radiol.* 31 (5) (2021) 3116–3126, <https://doi.org/10.1007/s00330-020-07361-z>.
- [45] X. Zhang, Z. Hua, R. Chen, et al., Identifying vulnerable plaques: A 3D carotid plaque radiomics model based on HRMRI, *Front Neurol.* 14 (2023) 1050899, <https://doi.org/10.3389/fneur.2023.1050899>.
- [46] S. Chen, C. Liu, X. Chen, W.V. Liu, L. Ma, Y. Zha, A radiomics approach to assess high risk carotid plaques: a non-invasive imaging biomarker, retrospective study, *Front Neurol.* 13 (2022) 788652, <https://doi.org/10.3389/fneur.2022.788652>.
- [47] U.R. Acharya, M.R.K. Mookiah, S. Vinitha Sree, et al., Atherosclerotic plaque tissue characterization in 2D ultrasound longitudinal carotid scans for automated classification: a paradigm for stroke risk assessment, *Med. Biol. Eng. Comput.* 51 (5) (2013) 513–523, <https://doi.org/10.1007/s11517-012-1019-0>.
- [48] U.R. Acharya, S. Vinitha Sree, M. Muthu Rama Krishnan, et al., Atherosclerotic risk stratification strategy for carotid arteries using texture-based features, *Ultrasound Med. Biol.* 38 (6) (2012) 899–915, <https://doi.org/10.1016/j.ultrasmedbio.2012.01.015>.

- [49] R.U. Acharya, O. Faust, A.P.C. Alvin, et al., Symptomatic vs. asymptomatic plaque classification in carotid ultrasound, *J. Med. Syst.* 36 (3) (2012) 1861–1871, <https://doi.org/10.1007/s10916-010-9645-2>.
- [50] U.R. Acharya, O. Faust, S. vs., et al., Understanding symptomatology of atherosclerotic plaque by image-based tissue characterization, *Comput. Methods Programs Biomed.* 110 (1) (2013) 66–75, <https://doi.org/10.1016/j.cmpb.2012.09.008>.
- [51] A. Chaudhry, M. Hassan, A. Khan, Robust segmentation and intelligent decision system for cerebrovascular disease, *Med. Biol. Eng. Comput.* 54 (12) (2016) 1903–1920, <https://doi.org/10.1007/s11517-016-1481-1>.
- [52] Z. Huang, X.Q. Cheng, H.Y. Liu, et al., Relation of carotid plaque features detected with ultrasonography-based radiomics to clinical symptoms, *Transl Stroke Res.* 13 (6) (2022) 970–982, <https://doi.org/10.1007/s12975-021-00963-9>.
- [53] E. Kyriacou, C.S. Pattichis, M.S. Pattichis, et al., Classification of atherosclerotic carotid plaques using gray level morphological analysis on ultrasound images, in: I. Maglogiannis, K. Karpouzis, M. Bramer (Eds.), *Artificial Intelligence Applications and Innovations. IFIP International Federation for Information Processing*, Springer, US, 2006, pp. 737–744, https://doi.org/10.1007/0-387-34224-9_87.
- [54] E. Kyriacou, A. Nicolaidis, C.S. Pattichis, First and second order statistical texture features in carotid plaque image analysis: Preliminary results from ongoing research, *IEEE 2011* (2011) 6655–6658, <https://doi.org/10.1109/IEMBS.2011.6091641>.
- [55] A. Lambrou, H. Papadopoulos, E. Kyriacou, et al., Evaluation of the risk of stroke with confidence predictions based on ultrasound carotid image analysis, *Int. J. Artif. Intell. Tools.* 21 (04) (2012) 1240016, <https://doi.org/10.1142/S0218213012400167>.
- [56] S. Latha, D. Samiappan, P. Muthu, R. Kumar, Fully automated integrated segmentation of carotid artery ultrasound images using DBSCAN and affinity propagation, *J. Med. Biol. Eng.* 41 (2) (2021) 260–271, <https://doi.org/10.1007/s40846-020-00586-9>.
- [57] B. Smitha, K.P. Joseph, A new approach for classification of atherosclerosis of common carotid artery from ultrasound images, *J. Mech. Med. Biol.* 19 (01) (2019) 1940001, <https://doi.org/10.1142/S0219519419400013>.
- [58] N. Tsiaparas, S. Golemati, I. Andreadis, J.S. Stoitsis, I. Valavanis, K.S. Nikita, Comparison of multiresolution features for texture classification of carotid atherosclerosis from B-mode ultrasound, *IEEE Trans. Inform. Technol. Biomed.* 15 (1) (2011) 130–137, <https://doi.org/10.1109/TITB.2010.2091511>.
- [59] X. Huang, Y. Zhang, M. Qian, et al., Classification of carotid plaque echogenicity by combining texture features and morphologic characteristics, *J. Ultrasound Med.* 35 (10) (2016) 2253–2261, <https://doi.org/10.7863/ultra.15.09002>.
- [60] L.M. Pedro, J.M. Sanches, J. Seabra, J.S. Suri, E. Fernandes, J. Fernandes, Asymptomatic carotid disease—a new tool for assessing neurological risk, *Echocardiography* 31 (3) (2014) 353–361, <https://doi.org/10.1111/echo.12348>.
- [61] E.P.V. Le, L. Rundo, J.M. Tarkin, et al., Assessing robustness of carotid artery CT angiography radiomics in the identification of culprit lesions in cerebrovascular events, *Sci Rep.* 11 (1) (2021) 3499, <https://doi.org/10.1038/s41598-021-82760-w>.
- [62] U. Acharya, S.V. Sree, M. Mookiah, et al., Computed tomography carotid wall plaque characterization using a combination of discrete wavelet transform and texture features: a pilot study, *Proc. Inst. Mech. Eng. H.* 227 (6) (2013) 643–654, <https://doi.org/10.1177/0954411913480622>.
- [63] S. Ali, F. Akhlaq, A.S. Imran, Z. Kastrati, S.M. Daudpota, M. Moosa, The enlightening role of explainable artificial intelligence in medical & healthcare domains: a systematic literature review, *Comput. Biol. Med.* 166 (2023) 107555, <https://doi.org/10.1016/j.cmpbiomed.2023.107555>.
- [64] Z. Sadeghi, R. Alizadehsani, M.A. Cifci et al., A Brief Review of Explainable Artificial Intelligence in Healthcare Published Online April 4, 2023, doi: 10.48550/arXiv.2304.01543.
- [65] N.M. Safdar, J.D. Banja, C.C. Meltzer, Ethical considerations in artificial intelligence, *Eur. J. Radiol.* 122 (2020) 108768, <https://doi.org/10.1016/j.ejrad.2019.108768>.
- [66] I. Cuocolo, Machine learning solutions in radiology: does the emperor have no clothes? *Eur. Radiol.* 31 (6) (2021) 3783–3785, <https://doi.org/10.1007/s00330-021-07895-w>.
- [67] A.P. Brady, E. Neri, Artificial intelligence in radiology—ethical considerations, *Diagnostics (basel)*. 10 (4) (2020) 231, <https://doi.org/10.3390/diagnostics10040231>.
- [68] C. Wang, J. Zhang, N. Lassi, X. Zhang, Privacy protection in using artificial intelligence for healthcare: Chinese regulation in comparative perspective, *Healthcare*. 10 (10) (2022) 1878, <https://doi.org/10.3390/healthcare10101878>.
- [69] N. Naik, B.M.Z. Hameed, D.K. Shetty, et al., Legal and ethical consideration in artificial intelligence in healthcare: who takes responsibility? *Front Surg.* 9 (2022) 862322 <https://doi.org/10.3389/fsurg.2022.862322>.
- [70] S.S.F. Yip, H.J.W.L. Aerts, Applications and limitations of radiomics, *Phys. Med. Biol.* 61 (13) (2016) R150, <https://doi.org/10.1088/0031-9155/61/13/R150>.
- [71] A. Zwanenburg, S. Leger, L. Agolli, et al., Assessing robustness of radiomic features by image perturbation, *Sci. Rep.* 9 (1) (2019), <https://doi.org/10.1038/s41598-018-36938-4>.
- [72] M. Shafiq-ul-Hassan, G.G. Zhang, K. Latifi, et al., Intrinsic dependencies of CT radiomic features on voxel size and number of gray levels, *Med. Phys.* 44 (3) (2017) 1050–1062, <https://doi.org/10.1002/mp.12123>.
- [73] A. Traverso, L. Wee, A. Dekker, R. Gillies, Repeatability and reproducibility of radiomic features: a systematic review, *Int. J. Radiat. Oncol. *biology*physics.* 102 (4) (2018) 1143–1158, <https://doi.org/10.1016/j.ijrobp.2018.05.053>.
- [74] J.E. van Timmeren, R.T.H. Leijenaar, W. van Elmpt, et al., Test-retest data for radiomics feature stability analysis: generalizable or study-specific? *Tomography.* 2 (4) (2016) 361–365, <https://doi.org/10.18383/j.tom.2016.00208>.
- [75] R.T.H. Leijenaar, S. Carvalho, E.R. Velazquez, et al., Stability of FDG-PET Radiomics features: an integrated analysis of test-retest and inter-observer variability, *Acta Oncol.* 52 (7) (2013) 1391–1397, <https://doi.org/10.3109/0284186X.2013.812798>.
- [76] S. Ho, K. Phua, L. Wong, W. Goh, Extensions of the external validation for checking learned model interpretability and generalizability, *Patterns.* 1 (2020) 100129, <https://doi.org/10.1016/j.patter.2020.100129>.
- [77] M. Porcu, R. Cau, J.S. Suri, L. Saba, Artificial intelligence- and radiomics-based evaluation of carotid artery disease, in: C.N. De Cecco, M. Van Assen, T. Leiner (Eds.), *Artificial Intelligence in Cardiothoracic Imaging. Contemporary Medical Imaging*, Springer International Publishing, 2022, pp. 513–523, https://doi.org/10.1007/978-3-030-92087-6_48.